



Monitoring Turbidity in San Francisco Estuary and Sacramento–San Joaquin Delta Using Satellite Remote Sensing

Christine M. Lee, Erin L. Hestir, Nicholas Tuffillaro, Brendan Palmieri, Shawn Acuña, Amye Osti, Brian A. Bergamaschi, and Ted Sommer

Research Impact Statement: Satellite remote sensing can be used to complement in situ measurements and monitoring of turbidity, in support of management interests around water quality and ecosystems assessments.

ABSTRACT: This study utilizes satellite data to investigate water quality conditions in the San Francisco Estuary and its upstream delta, the Sacramento–San Joaquin River Delta. To do this, this study derives turbidity from the European Space Agency satellite Sentinel-2 acquired from September 2015 to June 2019 and conducts a rigorous validation with in situ measurements of turbidity from optical sensors at continuous monitoring stations. This validation includes 965 matchup comparisons between satellite and in situ sensor data across 22 stations, yielding $R^2 = 0.63$ and 0.75 for Nephelometric Turbidity Unit and Formazin Nephelometric Unit (FNU) stations, respectively. This study then applies remote sensing to evaluate patterns in turbidity during the Suisun Marsh Salinity Control Gates Action (“Gates action”), a pilot study designed to increase habitat access and quality for the endangered Delta Smelt. The basic strategy was to direct more freshwater into Suisun Marsh, creating more low salinity habitat that would then have higher (and more suitable) turbidity than upstream river channels. For all seven acquisitions considered from June 29 to September 27, 2018, turbidity conditions in Bays and Sloughs subregions were consistently higher (and more suitable) (26–47 FNU) than what was observed in the upstream River region (13–25 FNU). This overall pattern was observed when comparing images acquired during similar tidal stages and heights.

(KEYWORDS: remote sensing; water quality; Suisun Marsh; San Francisco Estuary; turbidity; Delta Smelt.)

INTRODUCTION

The San Francisco Estuary and its Delta, the Sacramento–San Joaquin River Delta (SFE-SSJD), is considered the hub of California’s water supply system and part of one of the world’s biodiversity hotspots, home to a multitude of native fish, birds, and mammalian species. SFE-SSJD receives runoff from

over 40% of California’s land area and conveys up to 50% of California’s runoff (Conomos 1979; Nichols et al. 1986; USGS 2000). This system has been highly altered to meet California’s water supply needs and includes over 1,100 miles of levees and conveyance structures. The 2009 Delta Reform Act requires that the State of California manages the system to support the “co-equal goals” of water supply reliability and ecosystem health and restoration. However,

Paper No. JAWR-20-0076-P of the *Journal of the American Water Resources Association* (JAWR). Received June 23, 2020; accepted April 18, 2021. © 2021 American Water Resources Association. **Discussions are open until six months from issue publication.**

Terrestrial Hydrology, Earth Science Section (Lee), NASA Jet Propulsion Laboratory, California Institute of Technology Pasadena, California, USA; Department of Civil and Environmental Engineering (Hestir), University of California Merced, California, USA; College of Earth, Ocean, and Atmospheric Sciences (Tuffillaro), Oregon State University Corvallis, Oregon, USA; 34North (Palmieri; Osti), Truckee, California, USA; Bay-Delta Initiatives (Acuña), Metropolitan Water District of Southern California Sacramento, California, USA; California Water Science Center (Bergamaschi), U.S. Geological Survey Sacramento, California, USA; and California Department of Water Resources (Sommer), Sacramento, California, USA (Correspondence to Lee: christine.m.lee@jpl.nasa.gov).

Citation: Lee, C.M., E. Hestir, N. Tuffillaro, B. Palmieri, S. Acuña, A. Osti, B. Bergamaschi, and T. Sommer. 2021. “Monitoring Turbidity in San Francisco Estuary and Sacramento–San Joaquin Delta Using Satellite Remote Sensing.” *Journal of the American Water Resources Association* 1–15. <https://doi.org/10.1111/1752-1688.12917>.

climate change (Cloern et al. 2011) and other issues, such as sea level rise (Ustin et al. 2014), land subsidence (Ingbritsen et al. 2000), earthquakes (Wong et al. 2008), invasive species (Cohen and Carlton 1998; Hestir et al. 2008; Khanna et al. 2018), contaminants (Brooks et al. 2012), water diversions (Grimaldo et al. 2009), and altered hydrology (Hutton et al. 2015) represent other external stressors on this system, which have massive implications for water supply and ecosystems resiliency.

The *Hypomesus transpacificus*, known as the Delta Smelt, is considered as an icon of these competing issues. Delta Smelt experienced a precipitous decline in the 1980s, leading to its listing under the federal endangered species act, and another sustained decline in 2002, from which the population has not fully recovered (Hanak et al. 2013; Moyle et al. 2016). Turbidity, along with temperature and salinity, has been shown to be a key environmental control on the detection and survivability of Delta Smelt in the SFE-SSJD (Feyrer et al. 2007; Nobriga et al. 2008). Studies have found that changes in turbidity correspond with the migration of Delta Smelt (Grimaldo et al. 2009; Sommer et al. 2011) and that turbid water is a critical contributor to successful feeding as well as predation avoidance from other non-native fish species (Ferrari et al. 2014; Hasenbein et al. 2016; Schreier et al. 2016). It is also expected that climate change impacts, such as extended drought periods, would continue to degrade habitat conditions for Delta Smelt (Cloern et al. 2011; Wagner et al. 2011; Brown et al. 2013). The continued impacts on Delta Smelt and their habitat have served as the impetus for multi-lateral collaborations across federal, state, local, and other organizations to improve management of the SFE-SSJD resources to meet its co-equal goals. The implementation of the *Biological Opinions* released by NOAA and FWS, for example, mandates that water operations throughout the SFE-SSJD need to take into account turbidity and other water quality conditions as a way to minimize detrimental outcomes for the Delta Smelt (e.g., entrainment or habitat loss) (United States Fish and Wildlife Service 2019).

Current approaches for monitoring and managing water quality in SFE-SSJD depend heavily on in situ optical sensor measurements made across a network of fixed water quality stations as well as field surveys (Merz et al. 2011). There are 69 stations that record turbidity in 15-min or one-hour increments. Additionally, there are ongoing field surveys conducted by the United States (U.S.) Geological Survey (USGS) and California Department of Water Resources (CDWR). These data, however, provide a partial view into changes in water quality conditions and how they relate to species of concerns and their habitat quality.

Hydrodynamic models (Bever et al. 2018) or statistical approaches and interpolation (Greenberg et al. 2011) have also been used to fill in some spatial and temporal gaps. Datasets from satellite or airborne continue to be investigated (Fichot et al. 2016) but are underutilized overall as a supplement to an operational monitoring network.

Measurements of water column optical properties through the use of satellite or airborne remote sensing have the potential to increase the extent of in situ monitoring station networks or supplement such programs by orders of magnitude, and as summarized in Table 1. Measurement of turbidity is achieved by assessing optical properties within a water sample using spectrophotometric methods. In the laboratory or field, this is largely implemented using probes that are in direct contact with the water column or sample. When considering satellite-based detection, however, there are additional components to estimating turbidity that are associated with adjusting the remote sensing measurements to account for atmosphere (known as “atmospheric correction”) as well as modeling spectral data into a turbidity value. Atmospheric correction is a critical component of aquatic remote sensing, as the atmosphere is the greatest source of uncertainty in estimating surface reflectance over water (Salama and Stein 2009; IOCG 2010) and represents ~90% of the signal detect at-sensor.

This study is focused on enabling monitoring of turbidity characteristics across large and complex spatial domains by developing, testing, and implementing a satellite data processing workflow over the SFE-SSJD, which is ultimately being made accessible through the 34N baydeltalive.com portal (nasa.baydeltalive.com), along with the capacity to customize

TABLE 1. Summary of differences in data used in this study.

Summary of data sources	Temporal resolution	Spatial resolution	Spatial coverage
Water quality stations	15 min intervals (aggregated to 1 h)	Point data	69 stations (used 22 in this study) over 5,600 square miles
Sentinel-2A/B satellite data	five-day revisit 98 useable (cloud/smoke-free) acquisitions from September 2015–December 2019	20-m × 20-m pixels (average value over 20-m × 20-m)	¹ 36M+ pixels over 5,600 square miles

¹This number represents the upper limit of data pixels available, which could be sampled from, but may not be appropriate to use simultaneously due to spatial autocorrelation.

analyses, visualizations, and data dashboards. This work leverages ACOLITE, an open-source python package, that has developed and validated (and have improved upon) algorithms for satellite remote sensing of water quality (Nechad et al. 2009, 2010; Dogliotti et al. 2015; Vanhellemont and Ruddick 2016). This study evaluates satellite-derived turbidity using the fixed station data from the California Data Exchange Center ($N = 965$ points considered in total). As a test of the utility of our approach, we then apply the algorithm to evaluate regional differences in turbidity fields during a novel August 2018 management action, operation of the Suisun Marsh Salinity Control Gates, an effort to enhance Delta Smelt habitat (California Natural Resources Agency 2016). The details of this pilot flow study (henceforth, the “Gates action”) are described below.

METHODS

Satellite Data from Sentinel-2

Sentinel-2A/B (S2A or S2B) is an Earth observations mission that consists of a pair of satellites, each equipped with a multispectral imager, and was launched and is operated through the European Space Agency Copernicus Programme. S2 acquires data approximately every five days at higher spatial resolution (10, 20, and 60 m, depending on band). S2A was launched in June of 2015, and S2B followed in March of 2017. Both sensors make measurements in 12 spectral bands across the visible to shortwave infrared portion of the electromagnetic spectrum. This project utilizes four Sentinel-2 tiles for the region of interest, associated with the following tile IDs: T10SEG, T10SFH, T10SEH, and T10SFG. A summary of differences between in situ and satellite data sources is provided in Table 1.

Field Data — Fixed Water Quality Station Measurement

Fixed water quality station records were acquired through the California Data Exchange Center (<http://cdec.water.ca.gov>) by querying a database for turbidity data from September 2015 to June 2019, which overlaps with the majority of the Sentinel-2 data record. Probes on the continuous monitoring stations make measurements in Formazin Nephelometric Units (FNU) or in Nephelometric Turbidity Units (NTU). Both types of sensors are submersed in water and measure the amount of scattered light at 90°

from an incident light beam. FNU is measured with an infrared light source (ISO 7027, <https://www.iso.org/standard/69545.html>), whereas NTU is measured with a broadband (white) tungsten light source (USEPA 1993). FNU give an inherent optical property because it is not sensitive to the ambient light field and is thus more traceable to the bio-optical models that underpin many remote sensing approaches (Nechad et al. 2009; Dogliotti et al. 2015). Twenty-two stations (eleven stations measured in NTU; eleven stations measured in FNU) were used for this study and selected based on the availability of quality data for matchups. More details on how the 22 stations were identified, see subsection below (Satellite/Water [Ground] Observations Matchups). Furthermore, additional information on each station can be accessed through CDEC links, summarized in Figure S1.

Marine Surface Reflectance and Atmospheric Correction

Dark Spectrum Fitting (Vanhellemont 2019) within the ACOLITE platform (Vanhellemont and Ruddick 2016) was used to optimize atmospheric correction of Sentinel-2 imagery. Dark pixels are identified within a scene and used to generate a representative dark spectrum. Root mean squared error (RMSE) is computed for dark spectrum reflectance values and associated atmospheric path reflectance values from a look-up table (LUT), which also contains aerosol optical thickness, atmospheric spherical albedo, and two-way diffuse atmospheric transmittance. This LUT (Tanre et al. 1990; Kotchenova and Vermote 2007) is generated using the 6SV radiative transfer model with two aerosol models using a hyperspectral dataset and resampled to be applicable for Sentinel-2 and other multispectral sensors (Vanhellemont and Ruddick 2018). The LUT aerosol optical thickness values are used to filter combinations by band. The remaining model/band combination that yields a minimum RMSE is then used to generate water surface reflectance within the scene. A cloud mask was used to eliminate data acquired over clouds, which would otherwise saturate reflectance values and result in extreme overestimates of turbidity. Automated detection of water pixels over coastal and inland waters can be problematic due to a number of confounding factors. Among these are high turbidity, thin clouds over water, reflections from land features, shadows from clouds and land, particularly for inland water reservoirs in mountain areas. Even recent improvements to Landsat-8’s “Fmask,” with dynamic thresholding, often misidentifies water pixels in this region’s images, often due to high turbidity

(Luo et al. 2018). Therefore, a fixed land mask was created for the central images analyzed here using a combination of thresholding using near-infrared data combined with manual adjustments for misclassified pixels.

Turbidity Algorithm for S2

Previous studies have found reasonable agreement between turbidity derived from water surface reflectance over inland and coastal waters with in situ measurements and have documented a set of algorithms evaluated at sites around the world (Nechad et al. 2009; Dogliotti et al. 2015; Caballero et al. 2018; Kuhn et al. 2019) and represents one of the core capabilities of ACOLITE. Most of these algorithms are based on the principle that as the particle load in the water column increases, the water surface reflectance increases, and red shifts (Giardino et al. 2017), including in red or near-infrared bands to estimate particle load (Ruddick et al. 2006). This study heavily leverages these foundations, using the red band (Nechad et al. 2009) which, for Sentinel-2 corresponds with a band centered at 664 nm.

In this approach, turbidity is derived using a semi-empirical algorithm relating spectral reflectance to inherent optical properties (IOPs) absorption and backscatter:

$$\text{Turbidity}(T) = \frac{A_T \rho_w(\lambda)}{(1 - \rho_w(\lambda)/C^\lambda)} [\text{FNU}], \quad (1)$$

where A_T and C are wavelength-dependent calibration coefficients that encompass IOP characteristics. This study uses the red band ($\lambda = 664$ nm) implementation and maintains the default calibration coefficients noted in this study (Nechad et al. 2009), with future work to include updates utilizing in situ measurements or field-site specific IOPs.

Satellite/Water (Ground) Observations Matchups

To consistently compare in situ turbidity measurements from CDEC with derived values from S2, the datasets were aligned spatially and temporally. 3×3 window of pixels (totaling 60×60 m²) was sampled from each usable S2-derived turbidity raster, centering on the CDEC-registered latitude/longitude locations. Temporal sampling was achieved by sampling CDEC station data spanning one hour before to one hour after the Sentinel-2 overpass which generally occurred around 1100 local time (consistent with the three-hour window of the acquisition described

previously by Bailey and Werdell (2006). Additional data quality measures from Bailey and Werdell (2006) were implemented, including discarding pixels returning negative values and pixels that fell outside of one sigma of the 3×3 pixel means, which would minimize the inclusion of mixed or contaminated pixels. When applied to station data, this allowed erratic sensor measurements to be eliminated. Furthermore, matches were discarded if a spatial sample contained less than 5 of 9 pixels. Two additional quality control steps were taken by removing matches with stations that consisted of <10 matchups over the study period (2015–2019); we also visually identified two dates ($N = 15$) where it appeared the atmospheric correction algorithm failed and those points were removed.

The initial dataset consisted of 69 CDEC water quality stations which were filtered to 22 stations following data quality controls, with 11 stations measuring in NTU and 11 stations measuring in FNU (Figure 1; Table 2). Below, we evaluate Sentinel-2 derived turbidity by binning data into FNU reporting stations and NTU reporting stations. This study utilized a total of 965 matchups points during 2015–2019, of which $N = 522$ were used for S2 FNU vs. Fixed Stations (NTU) comparisons and $N = 443$ for S2 FNU vs. Fixed Stations (FNU). Stations sampled local turbidity at 15-min intervals, which were aggregated to an hour prior to and following the satellite. Aggregating temporally provided a means of evaluating variability in station data as well as provide a means of filtering out erroneous measurements, reflected in sudden or erratic changes in values.

Analysis of Turbidity during Suisun Marsh Salinity Control Gates Action (“Gates action”)

Overview. As a test application for this algorithm as an evaluation tool, we used this approach to examine water quality changes during a novel 2018 flow action to support Delta Smelt (California Natural Resources Agency 2016; Sommer et al. 2020). CDWR lead a pilot study in collaboration with multiple agencies. The goal of this effort was to increase freshwater flows and improve habitat quality, with outcomes assessed using multiple environmental parameters, including water quality, plankton, clams, and fish community changes. In this study, we introduce the use of remote sensing data as a supplement in understanding outcomes related to turbidity patterns during the Gates action.

The basic concept for the Gates action is as follows. Under typical low flow years, salinity intrusion during summer forces Delta Smelt out of Suisun Marsh and Bay (Figure 1), pushing the fish into narrower upstream river channels with less suitable habitat

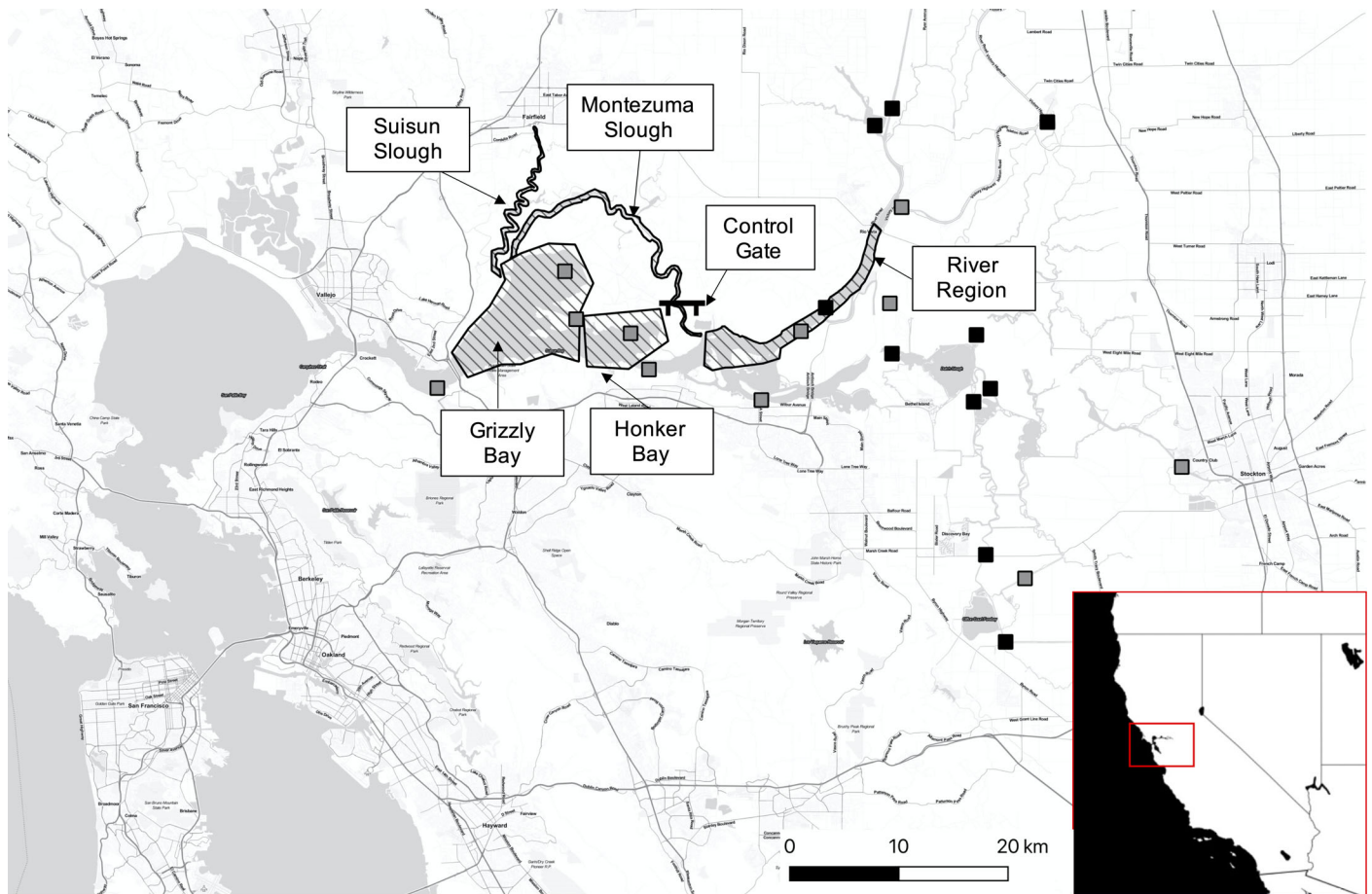


FIGURE 1. Study area for San Francisco Estuary and Sacramento–San Joaquin Delta, including locations of 22 CDEC fixed water quality stations, and subregions used to evaluate the Suisun Marsh Salinity Control Gates Action. Black boxes correspond with locations of 11 CDEC stations reporting in Formazin Nephelometric Unit [FNU]; grey boxes correspond with 11 CDEC stations reporting in Nephelometric Turbidity Unit [NTU].

(e.g., lower turbidity). To try and address this issue, CDWR tested a combination of an increase in freshwater inflow, coupled with the use of a unique water structure (Suisun Marsh Salinity Control Gates) to direct more low salinity water ($160 \times 10^6 \text{ m}^3$) into Suisun Marsh (“Gates action”) in August 2018. The goal of the Gates action was to allow Delta Smelt to colonize the Suisun Marsh during a time when it would otherwise be too salty, as is typically the case in a low flow year such as 2018. Based on prior continuous water quality data, CDWR predicted that the Suisun Marsh and surrounding subregions would have higher turbidities than the upstream River subregion (Figure 1), where Delta Smelt would have otherwise been confined. While CDWR did not expect that the action would change turbidity in any of the regions, we examined spatial and temporal patterns to see if there was evidence of differences following the action. Sommer and colleagues describe outcomes in more detail, observing an overall improvement in habitat quality with a focus on salinity and other

biological metrics (Sommer et al. 2020). The following sections describe our approach toward examining the variability of turbidity most likely associated with the Gates action while accounting for tidal stage and height.

Approach. First, image data were subset to regions of interest, which was latitudinally bounded by Grizzly Bay on the west and Rio Vista on the east; and longitudinally bounded by Honker Bay on the south to Belden’s Landing to the north (Figure 1). This resulted in a maximum of 2.3 million pixels per clear day acquisition that could be considered for the analysis. The Suisun Region of interest was then subdivided into four main subregions: (1) Grizzly Bay, (2) Honker Bay, (3) Marsh, including Montezuma Slough; and (4) River (Confluence to River) (Figure 1).

The Gates actions occurred between August 2 and September 6. This use case was evaluated over a timeframe of June 29 to September 27, which

TABLE 2. Table of 22 fixed water quality stations used in this study to evaluate Sentinel-2 derived turbidity. Total sample size = 965/
 $N = 522$ for CDEC stations (NTU) and $N = 443$ for CDEC stations (FNU).

Count	Sites	Sample size	Latitude	Longitude	Turbidity unit	Summary
1	ANH	27	38.01783	-121.80296	NTU	$N = 522$
2	GZB	25	38.123145	-122.00758	NTU	NTU stations = 11
3	GZL	74	38.12425	-122.03812	NTU	
4	HON	64	38.0724	-121.9392	NTU	
5	MAL	44	38.042805	-121.92009	NTU	
5	MRZ	38	38.027637	-122.14049	NTU	
6	RRI	32	37.963	-121.365	NTU	
7	RYC	63	38.083971	-121.99588	NTU	
8	SOI	46	38.17548	-121.65686	NTU	
9	SSI	53	38.074097	-121.76174	NTU	
10	TWI	45	38.0969	-121.6691	NTU	
11	VCU	26	37.8717	-121.5283	NTU	
12	DLC	32	38.245	-121.505	FNU	$N = 443$
13	DWS	67	38.25611	-121.66667	FNU	FNU stations = 11
14	FAL	52	38.0558	-121.6669	FNU	
15	GLC	22	37.8196	-121.5485	FNU	
16	HOL	23	38.0164	-121.5819	FNU	
17	LIB	48	38.2421	-121.6849	FNU	
18	OH4	26	37.891109	-121.56917	FNU	
19	ORQ	11	38.0272	-121.5645	FNU	
20	OSJ	47	38.0711	-121.5789	FNU	
21	PRI	63	38.0594	-121.5572	FNU	
22	SDI	50	38.0934	-121.736	FNU	

included four antecedent reference acquisitions (June 29, July 14, July 19, and July 24), two acquisitions during the Gates action (August 13, September 2) and one acquisition following the conclusion of the Gates action (September 27). This timeframe was established to help account for tidal influences as well as minimize variability that may arise due to seasonal trends. This study initially considered 19 Sentinel-2 images acquired during the period of June 29 to September 27, to include pre-Gates as well as post-Gates reference conditions. Of this initial 19-image set, nine images were discarded due to cloud contamination, and three were discarded due to smoke contamination from wildfires occurring in Northern California during that time (<https://www.fire.ca.gov/incidents/2018/>). The three images that were discarded due to cloud contamination were acquired in August, leaving only two clear-day images (August 13, 2018 and September 2, 2018) during the Gates action. The remaining seven images were used to assess changes in turbidity in terms of spatial and temporal variability.

Four of the seven images were binned by tidal stage and stage height, resulting in a separate sub-analysis of conditions during similar tidal conditions (June 29, July 14 for antecedent conditions; August 13 for conditions during the Gates action; and September 27 for post-Gate conditions). The tidal conditions for each day at the overpass time of Sentinel-2 were well-matched for antecedent (June 29 and

July 14, 2018; August 13 and September 2, 2018) and during-gates acquisitions during ebb entering low tide (0.44–0.53 m) and low tide entering slack (0.76 m) on September 27, 2018. For each of the sub-regions, all available pixels were aggregated within each subregion and averaged for the time series in, with images acquired during similar tidal stages labeled accordingly.

RESULTS

Satellite/In situ Matchups

Continuous Monitoring Station Matchups. During the study period (September 2015–June 2019), 98 acquisitions were able to be used for comparison and downstream analyses. These matches are displayed as a linear regression plot in Figure 2. S2-derived turbidity (FNU) matched close to a 1:1 line, with an offset of approximately 7 FNU ($R^2 = 0.75$). S2-derived turbidity (FNU) matched with in situ stations reporting in NTU) just below the 1:1 line (slope = 0.74) and a slightly greater offset of 14 and $R^2 = 0.63$, with summary statistics in Table 3.

Pearson's r values for both NTU and FNU stations indicate that Sentinel-2 derived turbidity and in situ values of turbidity are positively and linearly

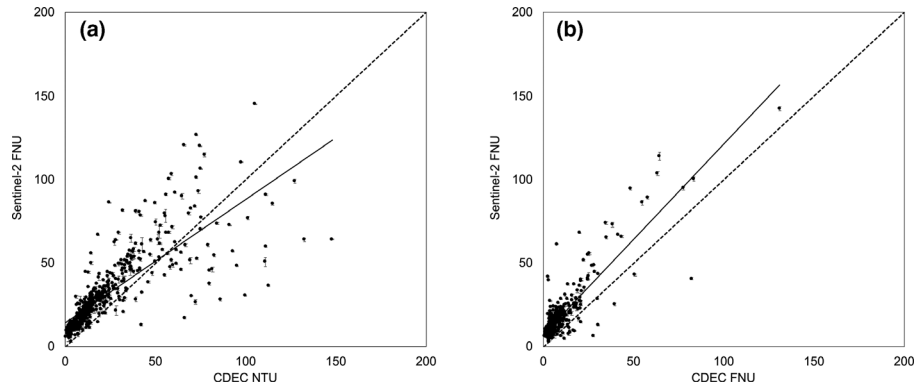


FIGURE 2. Comparing Sentinel-2 derived turbidity with CDEC station reported turbidity. (a) depicts S2 vs. CDEC (NTU) and (b) depicts S2 vs. CDEC (FNU). Vertical error bars reflect standard deviation over spatial domain (3×3 pixels from Sentinel-2). Note that many of the vertical error bars are smaller than the plot marker for Sentinel-2 turbidity values. Solid line represents the regression line and the dotted lines represent the 1:1 line.

TABLE 3. Summary statistics for each comparison from Figure 3.

In situ station type	Slope	Intercept	R^2 (p -value)	Pearson's r	RMSE	% Bias	MAE	Kendall's τ (p -value)
NTU $N = 522$	0.74	14	0.63 (<0.001)	0.79	17	34	12.6	0.76 (<0.001)
FNU $N = 443$	1.1	7	0.75 (<0.001)	0.87	11	87	8.82	0.53 (<0.001)

Notes: RMSE, root mean squared error; MAE, mean absolute error.

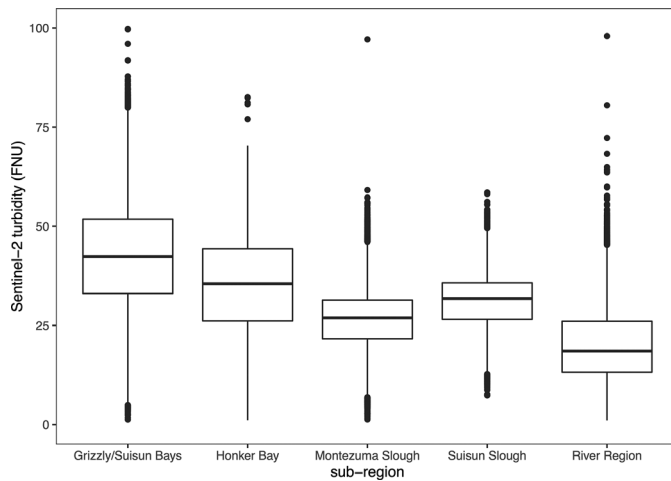


FIGURE 3. Boxplots of Sentinel-2 turbidity values by subregion.

correlated. The percent bias for FNU (87%) suggests that Sentinel-2 derived turbidity is likely to overestimate in situ for turbidity from CDEC stations reporting in FNU, with a regression slope of 1.1, indicating overestimation would be higher at higher turbidity values, and an offset of 7 FNU. NTU is less likely to overestimate (percent bias = 34%) but there is greater variance in estimates and $R^2 = 0.63$ and

larger offset (intercept = 14 FNU). This study also considers Kendall's τ , which is a nonparametric measure of relationships between ranked pairs; the calculated Kendall's τ suggests that S-2 FNU and CDEC NTU ($\tau = 0.76$) may be more strongly correlated than S2 FNU and CDEC FNU ($\tau = 0.53$).

Sentinel-2 Turbidity during the Suisun Marsh Salinity Control Gates Action

This study uses Sentinel-2 to assess differences in turbidity distributions across each of the subregions (Figure 1) and highlights turbidity field conditions during similar tidal stages and levels. Over the period of the Gates action, the overall distribution of turbidity values appears to differ by subregion (Figure 3); this is also visible when examining the five subregions over the Gates study period, depicted in Figure 4, and spanning June 29, 2018 to September 27, 2018. Figure 4 reflects substantial variability in the turbidity fields within Suisun Marsh area of interest. In addition to visual inspection of spatial variability of turbidity during the Gates actions, temporal changes across subregions were also assessed within subregions as defined by the hatched polygons in Figure 1. With all subregion estimates, it is important to keep in mind that the turbidity model RMSE

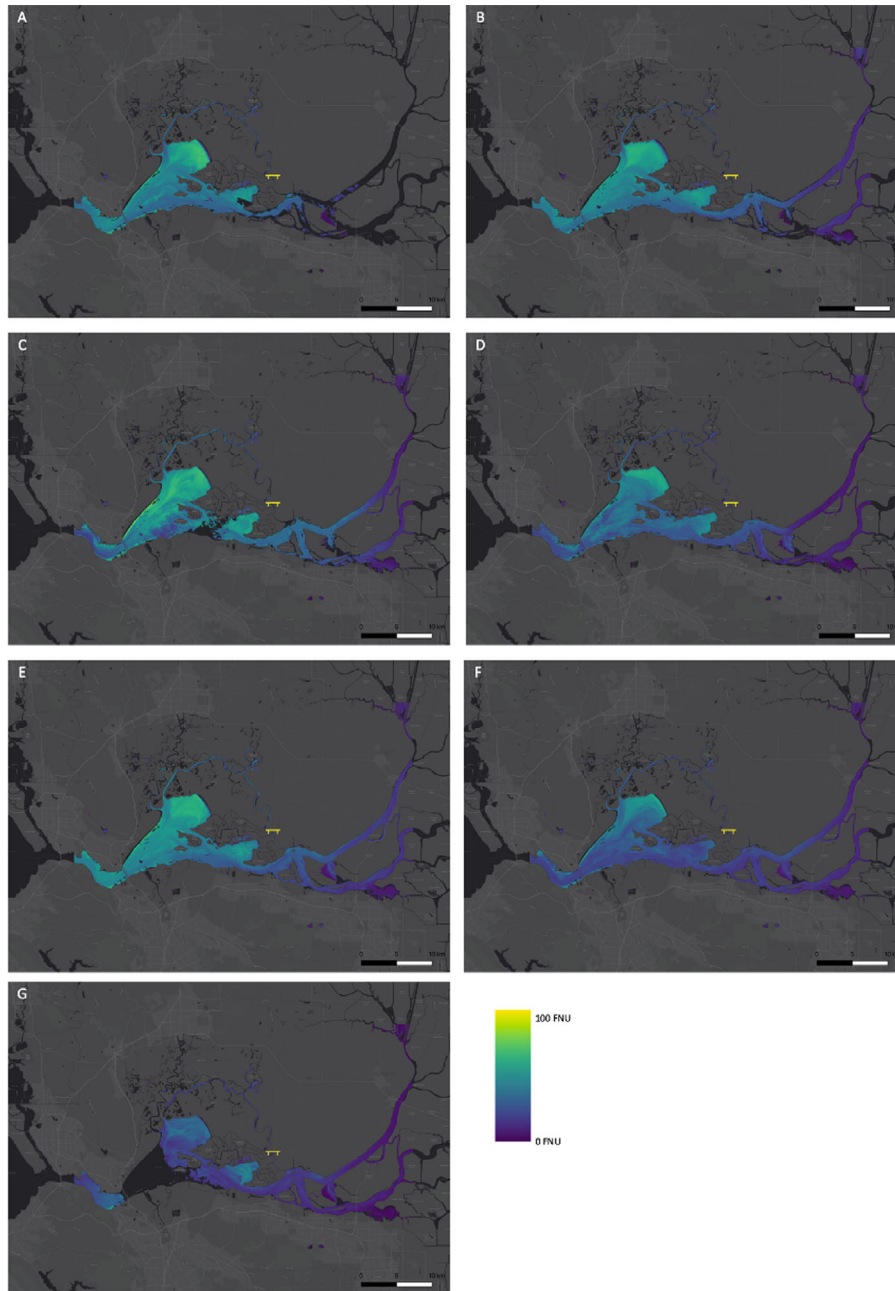


FIGURE 4. Sentinel-2 turbidity maps acquired prior to, during, and after the Gates action over subregions corresponding with Figure 1. (a) June 29, 2018; (b) July 14, 2018; (d) July 24, 2018; (e) August 13, 2018; (f) September 2, 2018; (g) September 27, 2018. Two images (e,f) were acquired during the Gates action. Black areas within the subregions (Figure 1) correspond with portions of the image masked due to cloud cover. Black areas within the image (outside of the subregions) are outside of the boundary of interest.

for FNU is 11 FNU. As predicted, the general pattern was lower turbidities in the upstream River subregion, and higher turbidities (and more favorable for Delta Smelt) in the downstream bay subregions including Suisun Marsh (Figures 3 and 4).

Bays. In Grizzly/Suisun and Honker Bays, this study leverages spatial maps of S2 turbidity to

evaluate changes in the turbidity over the region between June 29 and July 14 (Figure 5A, 5B). Average regional turbidity during the Gates action is shown to be slightly lower on August 13. Spatial averages of turbidity during the sample tidal stage are observed to be similar on June 29 and July 14, ranging from 46 ± 11 FNU to 47 ± 9 FNU in Grizzly/Suisun and 40 ± 9 FNU to 41 ± 9 FNU at Honker

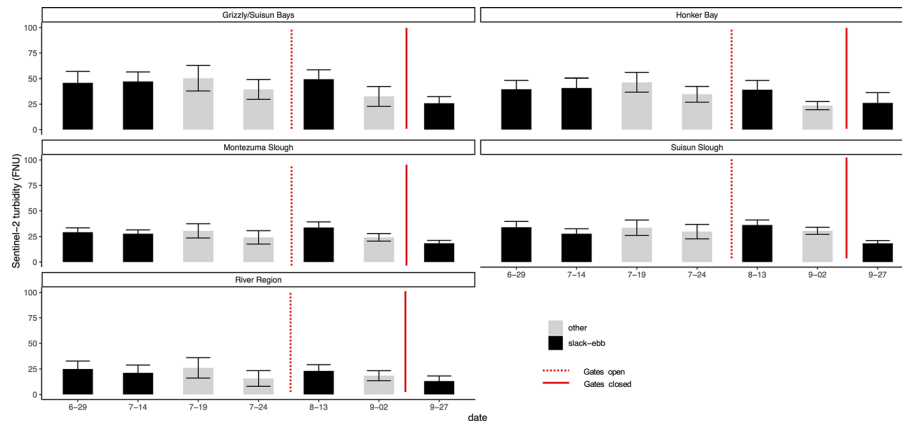


FIGURE 5. Time series plots of spatial averages of turbidity by subregion. Red bars denote period of Gates operation. Black columns denote conditions during the same tidal stage. Grey columns show conditions during other tidal stages.

Bay. While the average turbidity values changed, this change appears less than the standard deviation of the range of turbidity values sampled (9–11 FNU) as well as being less than the RMSE for FNU estimates (RMSE = 11 FNU). Following the Gates action, average turbidity conditions on 8/13 are higher than days prior to the Gates action — at 49 ± 9 FNU in Grizzly/Suisun and 38 ± 9 FNU in Honker. The greatest observed change in spatial averages of turbidity is a decrease in turbidity conditions on September 27 after the conclusion of the Gates action (26 ± 7 FNU in Grizzly/Suisun and 26 ± 10 FNU in Honker).

Sloughs. Regional average turbidity conditions are similar on June 29 and July 14, corresponding with 29 ± 4 FNU and 28 ± 4 FNU, respectively, at Montezuma Slough and 34 ± 6 FNU to 28 ± 5 FNU, respectively, at Suisun Slough (Figure 5C, 5D). Regional turbidity conditions observed during the Gates action, on August 13, were 34 ± 6 FNU at Montezuma and 36 ± 5 FNU for Suisun. After the Gates action concluded, regional turbidity values are shown to be 50%–52% lower on September 27, with 18 ± 3 FNU at Montezuma and 18 ± 3 FNU at Suisun. Conditions prior to and during the Gates action showed differences in spatial averages that are less than the variability of values within the turbidity field.

River Region. The River subregion, defined as the area from the confluence to Rio Vista, exhibits average turbidity conditions that are lower than the other sites on all dates during our study period (Figure 5E). Spatially averaged turbidity conditions are observed prior to the Gates action spanned 21 – 25 ± 8 FNU. Values observed during the Gates action on August 13, are within the range of variability

observed prior to the Gates, during similar tidal stages, at 23 ± 6 FNU. The minimum turbidity value in the River region among the dates with available data and throughout this time series is on September 27 at 13 ± 5 FNU.

DISCUSSION

Performance of Turbidity Algorithms in SFE

Previous work developing and implementing this algorithm (Nechad et al. 2009) has shown good performance when comparing satellite-derived turbidity values with in situ data, either derived by in situ radiometry and also matchups with measured turbidity values (Nechad et al. 2009; Dogliotti et al. 2015; Kuhn et al. 2019), occasionally with regional tuning and modifications (Caballero et al. 2018). In SFE-SSJD, there is an opportunity to build a fuller view of water quality conditions, and their potential impacts on the ecosystem, by leveraging fixed station networks and satellite data, and in conjunction with modeling. RMSEs observed between modeled turbidity utilizing S2 and measured in situ ranged from 11 for FNU matches and 17 for NTU matches. These are somewhat higher than other studies which have reported RMSE of 3.6–5.4 FNU (Dogliotti et al. 2016); however, Sentinel-2 estimates are assessing water surface conditions whereas CDEC stations are reported to be sampling at a 1-m depth and there can be considerable spatial lateral and vertical variability driven by local conditions. Dogliotti et al. 2015 reports an RMSE range of 5–33 FNU from sites around the world, though this study is implementing

a modified version of the algorithm originally reported (Nechad et al. 2009). Nechad et al. (2009) report an RMSE around ~5–7 FNU, relative to surface water sample measurements.

This study first utilizes spatial and temporal matching to evaluate ACOLITE turbidity products, which yield reasonably well-correlated matches with fixed water quality stations archived at CDEC (Figure 3). Because the atmosphere contributes ~90% of the signal received by the sensor, atmospheric correction over water can have a considerable impact on derived aquatic reflectance, which is then compounded when those reflectance values are used in water quality algorithms (Salama and Stein 2009; Kuhn et al. 2019). While not the focus of this study, the use of site-specific IOPs represents another opportunity to tune algorithms for improved estimates. For example, IOPs collected during field surveys could be used to update coefficients in the implementation of the turbidity algorithm depicted in Equation (1). Sources of uncertainty in this current implementation can be attributed to several sources, including differences in surface/subsurface conditions; remote sensing is measuring the integrated photic depth of the water column, and in situ stations have their sensors placed at approximately 1-m depth. For example, wind can result in significant differences in surface and subsurface conditions with respect to sediment supply and turbidity (Schoellhamer et al. 2007; Bever et al. 2018), as can tidal influences and flows (Cloern et al. 1989; Schoellhamer 2002; Kimmerer et al. 2015).

For the comparison between FNU estimates using Sentinel-2 data and CDEC NTU stations, inherent differences in how turbidity is estimated in FNU and NTU could also introduce uncertainties in these estimates. Future work may consider using satellite data to calibrate FNU to NTU stations within this system or to apply a systematic bias correction. Additional work to apply corrections to these estimates can utilize local biogeophysical parameters, such as wind speed, tidal stage, and flow which could help account for differences between surface and subsurface turbidity conditions. Future work will incorporate in situ spectral, probe, and water sample data collected during USGS cruises conducted coincident with satellite overpasses.

Delta Smelt and Gates Action

Delta Smelt is one of the highest-profile fishes in the U.S. because of its imperiled status and because its range overlaps with the water distribution for about 8% of the country's population and a multi-billion dollar agricultural industry (Robert F. Service

2007; Moyle et al. 2018). Many substantial water management and habitat activities are therefore required to try to protect and enhance the population. In addition, the State of California has voluntarily implemented additional actions to improve the status of the species (California Natural Resources Agency 2016). In this study, we examined the outcomes of one of these activities (the Gates action). Existing approaches for predicting and assessing outcomes associated with these recommendations rely primarily on in situ data collection, that are discrete in time and/or space, and modeling. Remote sensing represents an opportunity to supplement these tools for assessment with water quality parameters derived from remote sensing observations of conditions at the time of acquisition, with multiple orders of magnitude more data available on clear day acquisitions.

The goal of the Gates action was to direct more low salinity water into Suisun Marsh so as to allow Delta smelt to colonize that region during the critical summer period. In this manuscript, we point to the success of the Gates action, as documented by Sommer et al. 2020, whereby the Gates action improved habitat conditions for the Delta smelt in Suisun Marsh, which is well-known to be one of the most important habitats for this species (Hammock et al. 2017). Beneficial habitat features are hypothesized to include more complex hydrodynamics, increased food, and higher turbidity (Bever et al. 2018). CDWR expected that turbidity conditions in Bay and Marsh/Slough subregions were likely to remain favorable in terms of turbidity relative to the River region (Figure 1), which this study observed and verified, noting that pelagic bay regions remained favorable (>12 NTU) and exhibited very minimal changes (<3 FNU differences in turbidity average) during similar tidal conditions when comparing antecedent and during-Gates stages. We recognize that this difference of <3 FNU is within the standard deviation of the sampled area as well as lower than the RMSE. Similarly, in the marsh slough subregions, the turbidity averages observed during the Gates action were between the range of turbidity conditions observed prior to the Gates action. For all subregions the greatest change in average turbidity was observed following the conclusion of the Gates action on September 27 and this study does not explicitly account for seasonal drivers of turbidity changes.

It is important to note that this study works to maximize spatial data but has limited temporal coverage and is complementary to the temporally dense measurements from in situ stations. The River region, consistent with the hypothesis, had the lowest turbidity values, with the most substantial decreases (43%) observed when comparing August 13 (23 FNU) and September 27 (13 FNU). In an in-depth



Reservoir Conditions

The Bay Delta and Reservoir Conditions Map displays the most recent average turbidity and chlorophyll estimates for key water bodies across California. The values are derived from imagery acquired by Sentinel-2 and Landsat-8 satellites, which is then processed using automated algorithms on the NASA/BDL platform to produce fine resolution (20m), high spatial coverage water quality products. Real-time in-situ sensor data from the California Data Exchange Center is integrated into this summary map to describe current conditions including water temperature and reservoir capacity. Explore the data products, real-time conditions and management information for each reservoir by clicking on the corresponding reservoir page

[NASA Reservoir Conditions Map](#)

[View Map Gallery](#)

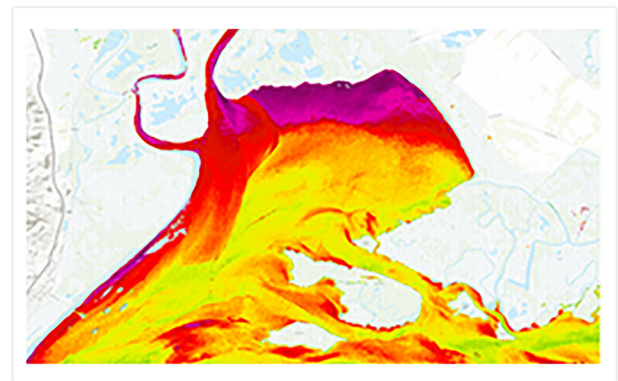


FIGURE 6. Bay Delta Live (<https://nasa.baydeltalive.com>) provides access to NASA Earth science data, in-situ monitoring stations, special studies in comprehensive dashboard format including maps, data visualization, map stories and collaborative workspaces.

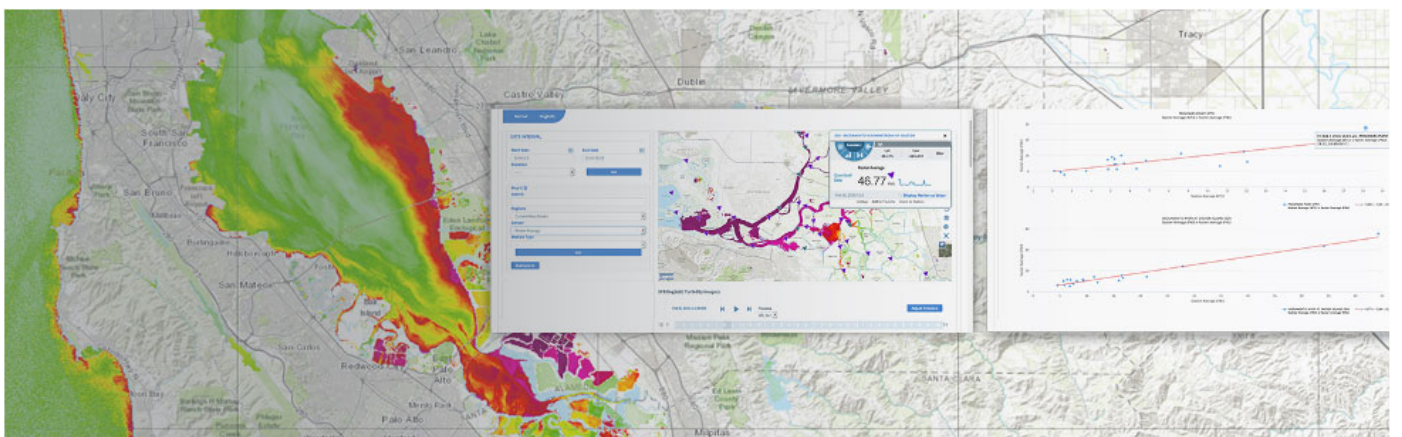


FIGURE 7. Interactive dashboard to visualize the results of the automated Sentinel-2 turbidity pipeline. Users can select which water quality parameter and remote sensing algorithm to display. Results are plotted on an interactive graph with correlation coefficients, standard deviation metrics, and best fit lines. Station data is also plotted spatial and available on the map interface.

evaluation of the outcomes of the Gates action, it was found that, consistent with this study, that turbidity did not show clear changes coincident with the Gates action, which was attributed to the strong dependency of turbidity conditions on wind-wave resuspension rather than tributary sediment inputs (Ruhl et al. 2001; Schoellhamer et al. 2007). Overall, the study found that the Gates action had a positive impact on physical habitat quality for the Delta Smelt, particularly as it relates to salinity (Sommer et al. 2020). It is also important to note that the S2 derived turbidity has an RMSE of 11 FNU and may be overestimating turbidity. However, the greatest difference in turbidity between regions occurs on 9/27, following the conclusion of the Gates action, with the River region being lower than the other regions. This time point also has lower turbidity across all regions when compared to earlier time points.

While not included in the time frame of this Gates action evaluation, it was also observed that the decline in turbidity conditions across all spatial subregions following the conclusion of the Gates action (9/27) persisted into October and November 2018 and points to how turbidity patterns in this region have a seasonal dependency though this was not the focus on this study. Remote sensing datasets facilitate comparisons of these changes across spatial scales, enabling an observations-based approach to comparing differences. Some of the limitations in the use of remote sensing data are the dependence on clear day acquisitions; this study was not able to use twelve scenes (out of nineteen total) because of cloud and aerosol contamination. As noted in the SMSCG initial report, it was important to optimize analyses and data collection so that we could associate changes in conditions due to the Gates action vs. those associated with seasonality, local meteorological conditions, flow conditions, and tidal variability. Even with limitations, the ability to sample across continuous spatial scales could enhance existing assessments of water quality outcomes associated with restoration and habitat quality improvement actions such as SMSCG, especially when considered in conjunction with CDEC, field sampling, and modeling investigations.

“Big data” in the form of Earth science mission datasets have a tremendous opportunity in terms of advancing understanding of environmental challenges at local, regional, and global scales. However, for these advances to be useful in a practical context, we must acknowledge and help address challenges associated with working with big data, including limitations with compute resources, software, and experience in dealing with larger Earth science datasets. While numerous and diverse barriers exist (Schaeffer et al. 2013; Lee et al. 2014), this project (along with other efforts supported by NASA Applied Sciences) is addressing technical

challenges by improving access, analysis, and visualization of Earth science data and information.

This work is integrated into a publicly accessible web platform through Bay Delta Live (BDL) (<https://nasa.baydeltalive.com>, Figure 6), which has over 50 data dashboards and data products aggregating environmental conditions, fisheries, and operations data for water and ecosystem management in California. The project has established a data dissemination and evaluation pipeline for Sentinel-2, Landsat, and ECOSTRESS satellite and spaceborne remote sensing data products, and will include surface temperature and chlorophyll. BDL’s web-based map tools are publicly and easily accessed for viewing, as well as for analysis and interaction with data (exploration, pixel, and zonal analysis) and enable widespread, easy data discovery and data interaction across multiple stakeholder groups.

Currently, BDL centralizes and synthesizes NASA Earth science data with datasets from federal, state, and local data providers including CDEC, USGS National Water Inventory System (NWIS), NOAA, U.S. Fish and Wildlife Service, and California Irrigation Management and Information Systems (CIMIS) in order to present a comprehensive picture of current water and ecosystems conditions in California. This platform provides further exploration of these data using maps and analytics (including validation), visualizations and analysis. BDL also has a comprehensive geospatial data catalogue with over 200 spatial datasets relevant to the SFE-SSJD. This project’s major objective is to make NASA Earth science data available to water resource managers and decision makers for real time and adaptive management-based project work. To do this, data are added to current decision frameworks and workflows and can be easily synthesized with other key operations, monitoring data, and models. The dashboards and analysis facilitate monitoring and management strategies for fisheries, water quality, regulatory policy, and water use (exports) that impact salvage of species of concern at pumping facilities in the southern Bay-Delta. Figure 7 depicts a dashboard used in this study for comparing turbidity retrievals from Sentinel-2 with CDEC station data.

CONCLUSIONS

1. Sentinel-2 acquires spatially continuous data over the SFE-SSJD every five days and can be used to estimate turbidity with good performance ($R^2 = 0.75$, $r = 0.87$ for CDEC [FNU] stations; $R^2 = 0.63$, $r = 0.79$ for CDEC [NTU]).

2. Sentinel-2 derived turbidity could potentially be used to enhance evaluation of outcomes from management actions, such as the Gates action.
3. Turbidity conditions across five subregions in the Suisun Marsh area, sampled at similar tidal stages and levels, were similar on days prior to the Gates action and during the Gates action; average turbidity conditions were much lower on September 27 at all sites.
4. Average turbidity conditions in the River subregion were less than those within subregions from Bays and Sloughs, which was consistent with the predictions for the action (California Department of Water Resources 2019; Sommer et al. 2020).

SUPPORTING INFORMATION

Additional supporting information may be found online under the Supporting Information tab for this article: Figure S1 provides links to more information about CDEC stations used in this study.

ACKNOWLEDGMENTS

We gratefully acknowledge support from NASA, through opportunity NNN16ZDA001N-A.37. The research was carried out at the Jet Propulsion Laboratory, California Institute of Technology, under a contract with the National Aeronautics and Space Administration. California Institute of Technology. Government sponsorship acknowledged. Copyright 2020. All rights reserved.

AUTHORS' CONTRIBUTIONS

Christine M. Lee: Conceptualization; data curation; formal analysis; funding acquisition; investigation; methodology; project administration; resources; supervision; validation; visualization; writing-original draft; writing-review & editing. **Erin Hestir:** Conceptualization; data curation; methodology; writing-review & editing. **Nicholas Tuffillaro:** Data curation; methodology; validation; writing-review & editing. **Brendan Palmieri:** Software; validation; visualization; writing-review & editing. **Shawn Acuña:** Conceptualization; writing-review & editing. **Amye Osti:** Conceptualization; data curation; resources; software; supervision; visualization; writing-review & editing. **Brian Bergamaschi:** Conceptualization; methodology; writing-review & editing. **Ted Sommer:** Writing-original draft; writing-review & editing.

LITERATURE CITED

- Bailey, S.W., and P.J. Werdell. 2006. "A Multi-Sensor Approach for the on-Orbit Validation of Ocean Color Satellite Data Products." *Remote Sensing of Environment* 102: 12–23.
- Bever, A.J., M.L. MacWilliams, and D.K. Fullerton. 2018. "Influence of an Observed Decadal Decline in Wind Speed on Turbidity in the San Francisco Estuary." *Estuaries and Coasts* 41: 1943–67.
- Brooks, M.L., E. Fleishman, L.R. Brown, P.W. Lehman, I. Werner, N. Scholz, C. Mitchelmore et al. 2012. "Life Histories, Salinity Zones, and Sublethal Contributions of Contaminants to Pelagic Fish Declines Illustrated with a Case Study of San Francisco Estuary, California, USA." *Estuaries and Coasts* 35: 603–21.
- Brown, L.R., W.A. Bennett, R.W. Wagner, T. Morgan-King, N. Knowles, F. Feyrer, D.H. Schoellhamer, M.T. Stacey, and M. Dettinger. 2013. "Implications for Future Survival of Delta Smelt from Four Climate Change Scenarios for the Sacramento–San Joaquin Delta, California." *Estuaries and Coasts* 36: 754–74.
- Caballero, I., G. Navarro, and J. Ruiz. 2018. "Multi-Platform Assessment of Turbidity Plumes during Dredging Operations in a Major Estuarine System." *International Journal of Applied Earth Observation and Geoinformation* 68: 31–41.
- California Department of Water Resources. 2019. <https://water.ca.gov/News/Blog/2019/Sept-19/Helping-endangered-fish-return-to-Suisun-Marsh>.
- California Natural Resources Agency. 2016. *Delta Smelt Resiliency Strategy*. 13 pp. Sacramento, CA: California Natural Resources Agency. <https://resources.ca.gov/CNRALegacyFiles/docs/Delta-Smelt-Resiliency-Strategy-FINAL070816.pdf>.
- Cloern, J.E., N. Knowles, L.R. Brown, D. Cayan, M.D. Dettinger, T.L. Morgan, D.H. Schoellhamer et al. 2011. "Projected Evolution of California's San Francisco Bay-Delta-River System in a Century of Climate Change." *PLoS One* 6: e24465.
- Cloern, J.E., T.M. Powell, and L.M. Huzzey. 1989. "Spatial and Temporal Variability in South San Francisco Bay (USA). II. Temporal Changes in Salinity, Suspended Sediments, and Phytoplankton Biomass and Productivity over Tidal Time Scales." *Estuarine, Coastal and Shelf Science* 28: 599–613.
- Cohen, A.N., and J.T. Carlton. 1998. "Accelerating Invasion Rate in a Highly Invaded Estuary." *Science* 279: 555–58.
- Conomos, T.J. 1979. *San Francisco Bay: The Urbanized Estuary. Investigations into the Natural History of San Francisco Bay and Delta; With Reverence to the Influence of Man*. San Francisco: Pacific Division/American Association for the Advancement of Science. https://www.waterboards.ca.gov/waterrights/water_issues/programs/bay_delta/deltaflow/docs/exhibits/ccwd/sprrt_docs/ccwd_conomos_1979.pdf#2thCHah-9ECwYA.
- Dogliotti, A.I., K.G. Ruddick, B. Nechad, D. Doxaran, and E. Knaeps. 2015. "A Single Algorithm to Retrieve Turbidity from Remotely-Sensed Data in All Coastal and Estuarine Waters." *Remote Sensing of Environment* 156: 157–68.
- Dogliotti, A.I., K. Ruddick, and R. Guerrero. 2016. "Seasonal and Inter-Annual Turbidity Variability in the Río de La Plata from 15 Years of MODIS: El Niño Dilution Effect." *Estuarine, Coastal and Shelf Science* 182: 27–39.
- Ferrari, M.C.O., L. Ranåker, K.L. Weinersmith, M.J. Young, A. Sih, and J.L. Conrad. 2014. "Effects of Turbidity and an Invasive Waterweed on Predation by Introduced Largemouth Bass." *Environmental Biology of Fishes* 97: 79–90.
- Feyrer, F., M.L. Nobriga, and T.R. Sommer. 2007. "Multidecadal Trends for Three Declining Fish Species: Habitat Patterns and Mechanisms in the San Francisco Estuary, California, USA." *Canadian Journal of Fisheries and Aquatic Sciences* 64: 723–34.
- Fichot, C.G., B.D. Downing, B.A. Bergamaschi, L. Windham-Myers, M. Marvin-DiPasquale, D.R. Thompson, and M.M. Gierach.

2016. "High-Resolution Remote Sensing of Water Quality in the San Francisco Bay-Delta Estuary." *Environmental Science & Technology* 50: 573–83.
- Giardino, C., M. Bresciani, F. Braga, I. Cazzaniga, L. De Keuke-laere, E. Knaeps, and V.E. Brando. 2017. *Bio-Optical Modeling of Total Suspended Solids. Bio-Optical Modeling and Remote Sensing of Inland Waters*. Amsterdam, Netherlands: Elsevier Inc.
- Greenberg, J.A., C. Rueda, E.L. Hestir, M.J. Santos, and S.L. Ustin. 2011. "Least Cost Distance Analysis for Spatial Interpolation." *Computers and Geosciences* 37: 272–76.
- Grimaldo, L.F., T. Sommer, N. Van Ark, G. Jones, E. Holland, P.B. Moyle, B. Herbold, and P. Smith. 2009. "Factors Affecting Fish Entrainment into Massive Water Diversions in a Tidal Freshwater Estuary: Can Fish Losses Be Managed?" *North American Journal of Fisheries Management* 29: 1253–70.
- Hammock, B.G., S.B. Slater, R.D. Baxter, N.A. Fanguie, D. Cocherell, A. Hennessy, T. Kurobe, C.Y. Tai, and S.J. Teh. 2017. "Foraging and Metabolic Consequences of Semi-Anadromy for an Endangered Estuarine Fish." *PLoS One* 12 (3): e0173497.
- Hanak, E., B. Jay Lund, B. John Durand, B. William Fleenor Brian Gray, B. Josué Medellín-Azuara, B. Jeffrey Mount Peter Moyle, B. Caitrin Phillips, and B. Barton. 2013. "Stress Relief: Prescriptions for a Healthier Delta Ecosystem." <https://www.ppic.org/>.
- Hasenbein, M., N.A. Fanguie, J. Geist, L.M. Komoroske, J. Truong, R. McPherson, and R.E. Connon. 2016. "Assessments at Multiple Levels of Biological Organization Allow for an Integrative Determination of Physiological Tolerances to Turbidity in an Endangered Fish Species. Conservation." *Physiology* 4: cow004.
- Hestir, E.L., S. Khanna, M.E. Andrew, M.J. Santos, J.H. Viers, J.A. Greenberg, S.S. Rajapakse, and S.L. Ustin. 2008. "Identification of Invasive Vegetation Using Hyperspectral Remote Sensing in the California Delta Ecosystem." *Remote Sensing of Environment* 112: 4034–47.
- Hutton, P.H., J.S. Rath, L. Chen, M.J. Unga, and S.B. Roy. 2015. "Nine Decades of Salinity Observations in the San Francisco Bay and Delta: Modeling and Trend Evaluations." *Journal of Water Resources Planning and Management* 142: 04015069.
- Ingbritsen, S.E., M.E. Ikehara, D.L. Galloway, and D.R. Jones. 2000. "Delta Subsidence in California." *Water Resources* 75: E66–72.
- IOOCG. 2010. "Atmospheric Correction for Remotely-Sensed Ocean Colour Products." In *International Ocean-Colour Coordinating Group Report*. Reports of the International Ocean-Colour Coordinating Group, No. 10, edited by M. Wang. Dartmouth: Canada.
- Khanna, S., M.J. Santos, J.D. Boyer, K.D. Shapiro, J. Bellvert, and S.L. Ustin. 2018. "Water Primrose Invasion Changes Successional Pathways in an Estuarine Ecosystem." *Ecosphere* 9: e02418.
- Kimmerer, W.J., M. MacWilliams, and E.S. Gross. 2015. "Variation of Fish Habitat and Extent of the Low-Salinity Zone with Freshwater Flow in the San Francisco Estuary." *San Francisco Estuary and Watershed Science* 11. <https://doi.org/10.15447/sfews.2013v11liss4art1>.
- Kotchenova, S.Y., and E.F. Vermote. 2007. "Validation of a Vector Version of the 6S Radiative Transfer Code for Atmospheric Correction of Satellite Data. Part II. Homogeneous Lambertian and Anisotropic Surfaces." *Applied Optics* 46: 4455–64.
- Kuhn, C., A. de Matos Valerio, N. Ward, L. Loken, H.O. Sawakuchi, M. Kampel, J. Richey *et al.* 2019. "Performance of Landsat-8 and Sentinel-2 Surface Reflectance Products for River Remote Sensing Retrievals of Chlorophyll-a and Turbidity." *Remote Sensing of Environment* 224: 104–18.
- Lee, C.M., T. Orne, and B. Schaeffer. 2014. "Remote Sensing of Water Quality: Bridging Operational and Applications Communities." *Eos, Transactions American Geophysical Union* 95: 354.
- Luo, Y., D. Doxaran, K. Ruddick, F. Shen, B. Gentili, L. Yan, and H. Huang. 2018. "Saturation of Water Reflectance in Extremely Turbid Media Based on Field Measurements, Satellite Data and Bio-Optical Modelling." *Optics Express* 26: 10435.
- Merz, J.E., S. HamMilton, P.S. BergmMan, and B. Cavallo. 2011. "Spatial Perspective for Delta Smelt: A Summary of Contemporary Survey Data." *California Fish and Game* 97: 164–89.
- Moyle, P.B., L.R. Brown, J.R. Durand, and J.A. Hobbs. 2016. "Delta Smelt: Life History and Decline of a Once-Abundant Species in the San Francisco Estuary." *San Francisco Estuary and Watershed Science* 14: <https://doi.org/10.15447/sfews.2016v14liss2art6>.
- Moyle, P.B., J.A. Hobbs, and J.R. Durand. 2018. "Delta Smelt and Water Politics in California." *Fisheries* 43: 42–50.
- Nechad, B., K.G. Ruddick, and G. Neukermans. 2009. "Calibration and Validation of a Generic Multisensor Algorithm for Mapping of Turbidity in Coastal Waters." In *Remote Sensing of the Ocean, Sea Ice, and Large Water Regions*. Berlin, Germany: SPIE, 74730H. <https://doi.org/10.1117/12.830700>
- Nechad, B., K.G. Ruddick, and Y. Park. 2010. "Calibration and Validation of a Generic Multisensor Algorithm for Mapping of Total Suspended Matter in Turbid Waters." *Remote Sensing of Environment* 114: 854–66.
- Nichols, F.H., J.E. Cloern, S.N. Luoma, and D.H. Peterson. 1986. "The Modification of an Estuary." *Science* 231: 567–73.
- Nobriga, M.L., T.R. Sommer, F. Feyrer, and K. Fleming. 2008. "Long-Term Trends in Summertime Habitat Suitability for Delta Smelt, *Hypomesus transpacificus*." *San Francisco Estuary and Watershed Science* 6. <https://doi.org/10.15447/sfews.2008v6liss1art1>.
- Robert F. Service. 2007. "Delta Blues, California Style." *Science* 317: 442–45.
- Ruddick, K.G., V. De Cauwer, Y.J. Park, and G. Moore. 2006. "Seaborne Measurements of near Infrared Water-Leaving Reflectance: The Similarity Spectrum for Turbid Waters." *Limnology and Oceanography* 51: 1167–79.
- Ruhl, C.A., D.H. Schoellhamer, R.P. Stumpf, and C.L. Lindsay. 2001. "Combined Use of Remote Sensing and Continuous Monitoring to Analyse the Variability of Suspended-Sediment Concentrations in San Francisco Bay, California." *Estuarine, Coastal and Shelf Science* 53: 801–12.
- Salama, M.S., and A. Stein. 2009. "Error Decomposition and Estimation of Inherent Optical Properties." *Applied Optics* 48: 4947–62.
- Schaeffer, B.A., K.G. Schaeffer, D. Keith, R.S. Lunetta, R. Conmy, and R.W. Gould. 2013. "Barriers to Adopting Satellite Remote Sensing for Water Quality Management." *International Journal of Remote Sensing* 34: 7534–44.
- Schoellhamer, D.H. 2002. "Variability of Suspended-Sediment Concentration at Tidal to Annual Time Scales in San Francisco Bay, USA." *Continental Shelf Research* 22: 1857–66.
- Schoellhamer, D.H., T.E. Mumley, and J.E. Leatherbarrow. 2007. "Suspended Sediment and Sediment-Associated Contaminants in San Francisco Bay." *Environmental Research* 105: 119–31.
- Schreier, B.M., M.R. Baerwald, J.L. Conrad, G. Schumer, and B. May. 2016. "Examination of Predation on Early Life Stage Delta Smelt in the San Francisco Estuary Using DNA Diet Analysis." *Transactions of the American Fisheries Society* 145: 723–33.
- Sommer, T., R. Hartman, M. Koller, M. Koohafkan, J.L. Conrad, M. MacWilliams, A. Bever, C. Burdi, A. Hennessy, and M. Beakes. 2020. "Evaluation of a Large-Scale Flow Manipulation to the Upper San Francisco Estuary: Response of Habitat Conditions for an Endangered Native Fish." *PLoS One* 15: e0234673.
- Sommer, T., F.H. Mejia, M.L. Nobriga, F. Feyrer, and L. Grimaldo. 2011. "The Spawning Migration of Delta Smelt in the Upper San Francisco Estuary." *San Francisco Estuary and Watershed Science* 9: 1–16.
- Tanre, D., J.L. Deuze, M. Herman, R. Santer, and E. Vermote. 1990. "Second Simulation of the Satellite Signal in the Solar

- Spectrum -6S Code.” *Digest — International Geoscience and Remote Sensing Symposium (IGARSS)* 35: 187.
- United States Fish and Wildlife Service. 2019. “Water Operations Biological Opinions, Bay-Delta Fish & Wildlife Office, USFWS.” <https://www.fws.gov/sfbaydelta/cvp-swp/index.htm>.
- USEPA. 1993. *Method 180.1: Determination of Turbidity by Nephelometry*. US EPA Office of Research and Development. https://www.epa.gov/sites/production/files/2015-08/documents/method_180-1_1993.pdf.
- USGS. 2000. *Delta Subsidence in California: The Sinking Heart of the State*. Reston, VA: USGS. <https://pubs.er.usgs.gov/publication/fs00500>, <https://doi.org/10.3133/fs00500>.
- Ustin, S.L., M.J. Santos, E.L. Hestir, S. Khanna, A. Casas, and J. Greenberg. 2014. “Developing the Capacity to Monitor Climate Change Impacts in Mediterranean Estuaries.” *Evolutionary Ecology Research* 16: 529–50.
- Vanhellemont, Q. 2019. “Adaptation of the Dark Spectrum Fitting Atmospheric Correction for Aquatic Applications of the Landsat and Sentinel-2 Archives.” *Remote Sensing of Environment* 225: 175–92.
- Vanhellemont, Q., and K. Ruddick. 2016. *Acolite for Sentinel-2: Aquatic Applications of MSI Imagery*. Paris, France: European Space Agency.
- Vanhellemont, Q., and K. Ruddick. 2018. “Atmospheric Correction of Metre-Scale Optical Satellite Data for Inland and Coastal Water Applications.” *Remote Sensing of Environment*. <https://doi.org/10.1016/j.rse.2018.07.015>.
- Wagner, R.W., M. Stacey, L.R. Brown, and M. Dettinger. 2011. “Statistical Models of Temperature in the Sacramento–San Joaquin Delta under Climate-Change Scenarios and Ecological Implications.” *Estuaries and Coasts*. <https://doi.org/10.1007/s12237-010-9369-z>.
- Wong, I., P. Thomas, J. Unruh, K. Hanson, and R. Youngs. 2008. *Characterizing the Earthquake Ground Shaking Hazard in the Sacramento–San Joaquin Delta, California*. Geotechnical Special Publication. [https://doi.org/10.1061/40975\(318\)170](https://doi.org/10.1061/40975(318)170).